# Simulation of Large Bubble/Molten Steel Interaction for Gas-Injected Ladle

*S.-M. Pan, J.-D. Chiang, and W.-S. Hwang*

*(Submitted 2 May 1997; in revised form 29 October 1998)*

**A mathematical model has been developed to simulate numerically the interactions between gas bubbles and molten steel during the gas-injection treatment in secondary refining of steel and to experimentally verify the reliability of the model. A marker-and-cell (MAC) technique is employed to simulate the motions of gas bubbles and molten steel. Photographic observation is used to evaluate the reliability of the mathematical model. A two-dimensional ladle with only one bubble was used to test the capability of the model to handle the interaction between the relatively large bubble and the molten steel. The shape of the bubble is initially round. Then it gradually becomes flattened and eventually evolves into a spherical-cap bubble. Molten steel is induced to flow and forms two circulations. The model was then tested on the same ladle with bubbles continuously released. The first bubble rises in a similar way as the previous case. The second bubble is affected by the first bubble and becomes slightly elongated in the vertical direction rather than in the horizontal direction. It also rises faster and later collides with the first bubble. The released bubbles can be grouped in clusters and are repeated cluster after cluster. Water-model experimental observations are consistent with the predicted results.**

**Keywords** gas bubbles, gas-injection treatment, marker-and-cell technique, water modeling

## 1. Introduction

To improve steel quality and simplify operating procedures, the steelmaking process is divided into two stages (Ref 1): (1) primary steelmaking in a furnace to produce raw steel and (2) secondary steelmaking in a ladle with various refining treatments. In recent years, the treatment of blowing argon gas in the refining ladle has been widely used for desulfurization, degassing, minor composition adjustment, temperature homogenization, and inclusion removal (Ref 2). As the gas bubbles are introduced into the ladle, they rise through the molten steel and cause the molten steel to flow. The flow of molten steel then affects how gas bubbles float. Because of the interactive flow, the additives, either desulfurization agents or alloying elements, can be mixed more effectively with the molten steel. Also, degassing and temperature homogenization can be achieved more readily. However, the treatment also causes several problems including reoxidation of the molten steel, slag entrapment, nitrogen pickup, refractory erosion, and cost increase. It is then desirable to understand the interactive flow phenomena of molten steel and gas bubbles under various conditions to optimize the operation of the treatment.

There are basically two types of gas-introducing treatments: gas-stirring treatment and gas-injection treatment. Schematic diagrams for the two treatments are shown in Fig. 1 and 2. The gas-stirring treatment usually blows only gas into the ladle. The gas-injection treatment, however, introduces the argon gas along with the solid additives into the system. Therefore, the gas is used not only to cause the molten steel to flow, but to act as the carrier gas. The two treatments are similar in that gas bubbles and molten steel interact with each other. However, the interactions differ in several ways. The gas bubbles in the stirring treatment are relatively large in number and small in size. The injection treatment, however, has fewer bubbles, but they are larger. During the bubble flotation, the shape of the smaller bubble remains unchanged while the larger bubble is severely deformed.

In the literature, a number of investigations have been conducted with mathematical and/or water models to understand the characteristics of fluid flow, heat transfer, and mass-transfer phenomena in gas-stirred ladles (Ref 3-10). In earlier studies (Ref 3-6), the size and shape of the plume zone where molten steel and gas bubbles coexist as well as the shearing force of the plume zone on the remaining molten steel zone

**S.-M. Pan, J.-D. Chiang,** and **W.-S. Hwang,** Department of Materials Science and Engineering, National Cheng Kung University, Tainan, Taiwan, R.O.C.

**Nomenclature**

| | |
|---|---|
| $g$ | gravity |
| $N_G$ | The number of gas particles in every computational cell |
| $P$ | pressure |
| $R_b$ | Bubble diameter |
| $U_m$ | Velocity of marker particle |
| $U, V$ | Velocity vector of the liquid in $X$, $Y$ direction, respectively |
| $V_\infty$ | Terminal velocity |
| $X_m^n$ | Old position of the marker |
| $X_m^{n+1}$ | New position of the marker |
| $\mu$ | Molecular viscosity |
| $\rho_f$ | Density of fluid |
| $\rho_G$ | Density of gas |
| $\rho_L$ | Density of liquid |
| $\sigma$ | Surface tension |

where only molten steel exists had been assumed/prescribed. Fluid-dynamics principles for the pure liquid were applied in the liquid zone to calculate the induced velocity field of the molten steel. Then, improvements were made to alleviate the necessity of prescribing the plume zone (Ref 7-10). In these studies, the complete ladle system, including the plume zone and the pure liquid zone, was considered simultaneously. A pseudo-single-phase model was usually employed to treat the two-phase flow system. The fluid in the system was considered to have only one phase, which is the mixture of gas and molten steel. A parameter, called liquid fraction—which is the percentage of a control volume occupied by liquid, was used in the model so that one set of fluid dynamics equations was enough to describe the flow behaviors in the plume zone where gas and molten steel coexist and in the liquid zone where only molten steel exists. While the numerical simulation of the flow phenomena in gas-stirred ladles was rather successful, it was also realized that the mathematical treatment could only handle the cases where the gas bubbles are considerably smaller than the meshing elements generated in the system for numerical simulation. This is unfortunately not the case for gas-injection operation where the gas bubbles are rather large compared to the meshing elements.

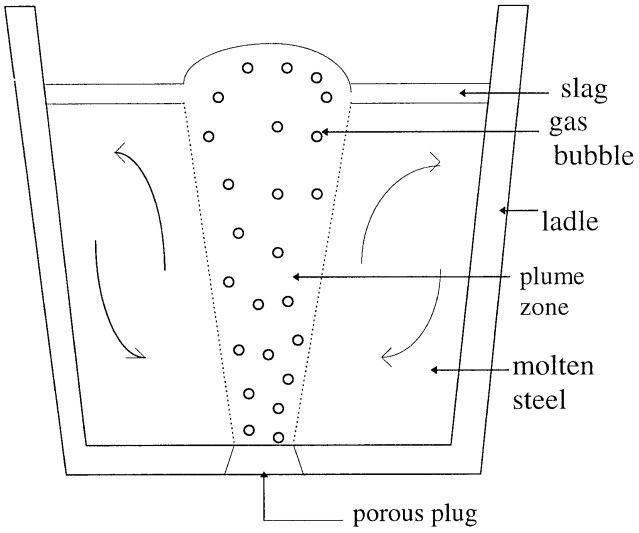


**Fig. 1** Diagram of the gas-stirring treatment

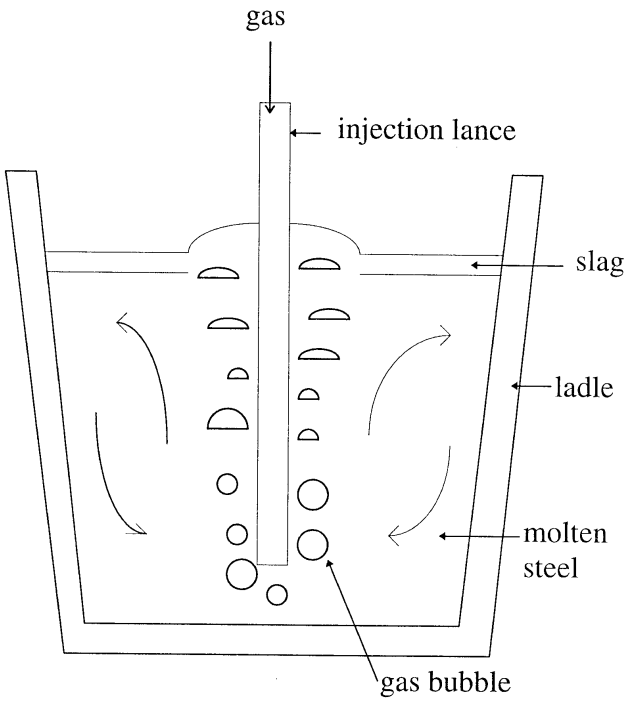


**Fig. 2** Diagram of the gas-injection treatment

For gas-injection treatment, two approaches have been employed to study the fluid-flow phenomena. One is the experimental approach. A number of studies had been conducted to measure experimentally and observe the variation of the bubble shape during its flotation, the initial motion and terminal velocity of the rising bubble (Ref 11-13), the bubble diameter, the volume fraction of the gas, and the released frequency of the gas bubbles in the plume zone (Ref 14-17). There were also studies of the mixing efficiency with respect to the various injection conditions in the ladle (Ref 18). The other approach is to use the numerical-simulation technique. Several computational fluid-dynamics techniques that have the capability to treat the gas/liquid interface problem have been applied to simulate numerically the gas/liquid interaction in the gas-injected ladle. The techniques include the volume-of-fluid (VOF) method (Ref 19, 20), the front tracking method (Ref 21), the projection method (Ref 22), and the marker-and-cell (MAC) method (Ref 23). While these studies succeeded in simulating the gas/liquid interactions when large bubbles are involved, they were, however, limited to the cases where only one bubble is floating in the ladle.

The purpose of this study was to develop a mathematical model that is capable of numerically simulating the two-phase fluid-flow phenomenon in the gas-injection operation of the secondary refining process in steelmaking and to verify experimentally the reliability of the mathematical model with a water model. The MAC technique was employed in this study (Ref 24). Only two-dimensional cases were considered. The concerned two-phase fluid flow included how the flotation of released bubbles induced the molten steel to flow, how the shapes of the bubbles vary during the flotation under the influence of the molten steel flow, and how the various bubbles interact with one another.

## 2. Mathematical Model

### *2.1 Description of the Physical Phenomena and the Mathematical Treatment*

The gas-injected ladle is essentially a gas-bubble-driven recirculating flow system. When argon gas is released from the injection lance, it forms rather large gas bubbles. Owing to the density difference, the gas bubbles tend to flow to the top. As they float, they induce the molten steel to flow, and in turn the flowing melt affects the rising patterns of the bubbles. It should be noted that during gas-injection operation, the size of the gas bubbles is rather large and the number of bubbles is rather small. It is therefore characteristic of the gas-injection treat-

ment that the effect of each individual bubble on the melt flow is quite significant, and the interactions among various gas bubbles are very important in affecting how the molten steel is induced to flow and how the gas bubbles rise to the surface. Meanwhile, the shape and speed of the rising bubbles keep changing, and the way they change may vary from one bubble to another. It was the purpose of this study to be able to simulate these phenomena.

In order to simulate numerically the fluid-flow phenomena in a gas-injected ladle, the system is first divided into a number of elements, called cells. A set of markers of the first kind is introduced in the system to represent the molten steel initially at rest. Then another set of markers of a second kind is used in the system to represent the introduction of the first gas bubble. The next step is to solve the partial differential equations that describe the fluid-flow behaviors of the fluid in each cell of the system. It should be noted that the cells may contain only liquid, or only gas, or a mixture of gas and liquid. In this study, a parameter called density function is incorporated in the partial differential equations to make the same set of equations applicable to all the elements. As the velocity of each cell is calculated, the marker velocity for either a liquid marker or a gas marker is then interpolated from these cell velocities. All the markers are moved according to their velocities, and a new flow condition is realized. The flow condition includes the velocity of the molten steel as well as the positions and shapes of the gas bubbles. By the gas-injection rate and the bubble-formation rate, a second bubble is formed later. Then, a set of markers of the second kind is introduced to represent its existence. The procedures are repeated until the flow system reaches its steady state.

### 2.2 Governing Differential Equations

As described earlier, the phenomenon discussed here is basically a two-phase fluid-flow phenomenon. However, only one set of governing differential equations is used to describe its fluid-flow behavior by employing a density function in the equations. The forms of the equations are as follows:

**Continuity Equation**

$$\frac{\partial U}{\partial X}+\frac{\partial V}{\partial Y}=0 \qquad \text{(Eq 1)}$$

**Momentum Equations**

$$\rho\left(\frac{\partial U}{\partial t}+U\frac{\partial U}{\partial X}+V\frac{\partial U}{\partial Y}\right)= -\frac{\partial P}{\partial X}+\frac{\partial}{\partial X}\left[\mu\left(\frac{\partial U}{\partial X}+\frac{\partial U}{\partial X}\right)\right]+\frac{\partial}{\partial Y}\left[\mu\left(\frac{\partial U}{\partial Y}+\frac{\partial V}{\partial X}\right)\right] \qquad \text{(Eq 2)}$$

$$\rho\left(\frac{\partial V}{\partial t}+U\frac{\partial V}{\partial X}+V\frac{\partial V}{\partial Y}\right)= -\frac{\partial P}{\partial Y}+\frac{\partial}{\partial X}\left[\mu\left(\frac{\partial V}{\partial X}+\frac{\partial U}{\partial Y}\right)\right]+\frac{\partial}{\partial Y}\left[\mu\left(\frac{\partial V}{\partial Y}+\frac{\partial V}{\partial Y}\right)\right]+\rho g \qquad \text{(Eq 3)}$$

where $\rho$ is the density of the control element and

$$\rho=\rho_G\,\delta(x,y)+\rho_L\,(1-\delta(x,y)) \qquad \text{(Eq 4)}$$

and $\delta(x,y)=1$, if $N_G\neq 0$; $\delta(x,y)=0$, if $N_G=0$.

### 2.3 Initial and Boundary Conditions

The initial condition is that the liquid is at rest and a spherical bubble of prescribed size appears at the opening of the injection lance. The wall-boundary condition used in this study was the free-slip boundary condition. The boundary conditions on the free surface of the liquid are that the tangential stress is zero and the normal stress equals the externally applied pressure.

### 2.4 Particle Velocity Calculation

In this study, an explicit finite-difference method was used to solve Eq 1 to 3 for the velocity and pressure of every cell in the ladle. Gas markers and liquid markers were used to represent the existing conditions of the gas bubbles and molten steel, respectively. It was then necessary to determine the velocities of the particles based on the velocities of the cells. An area-weighted method was used in this study to calculate the velocity of marker particle based on its neighboring-cell velocities as shown in Fig. 3:

$$U_m=\frac{A_1U_1+A_2U_2+A_3U_3+A_4U_4}{dx\,dy} \qquad \text{(Eq 5)}$$

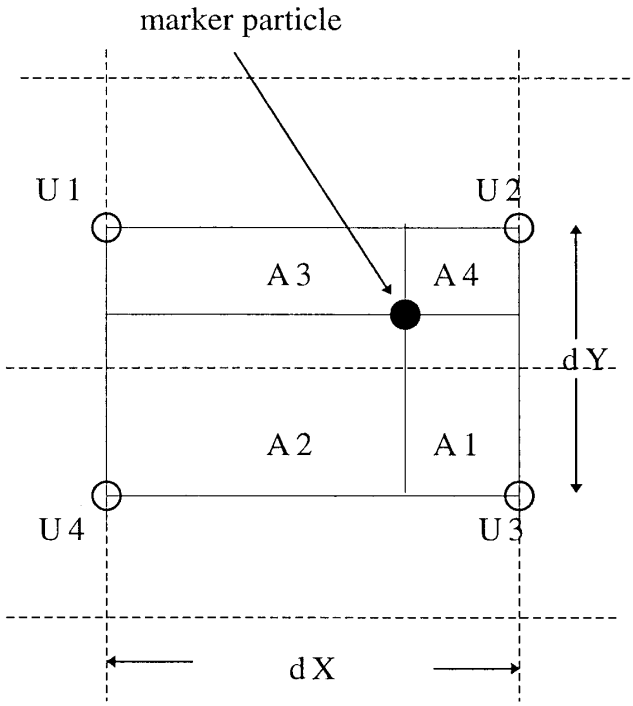


**Fig. 3** How a marker velocity is determined by the neighboring cell velocities

As the velocity of the marker particle was obtained, the new position of the marker was calculated according to:

$$X_m^{n+1} = X_m^n + U_m \times \delta t \quad \text{(Eq 6)}$$

### 2.5 Terminal Velocity of the Gas Bubble During Flotation

In gas-injection process, as the gas bubble is introduced into the liquid it rises in the molten steel due to the density difference. It is first accelerated under the influence of the buoyancy force. Then, the drag force of the liquid on the bubble motion gradually catches up. As the two forces balance, the gas bubble rises in a steady velocity, called the terminal velocity. In this study, it was also desirable to investigate the effect of gas bubble size on its terminal velocity during flotation. A study by Haberman and Morton shows that the terminal velocity of a gas bubble depends on its size; this relationship is shown in Fig. 4 (Ref 17). The figure clearly shows that the relationship can be divided into two categories. In zone A, the relationship between the terminal velocity and the size of a gas bubble exhibits a linear relationship. It is also known that in zone A, the bubble motion is very much affected by the surface tension and viscosity of the liquid and that the shape of the gas bubble remains spherical during flotation. The range of the bubble size corresponds to the gas-stirring conditions. In zone B, the relationship between the terminal velocity and the size of a gas bubble is very different. In this range of bubble size, the terminal velocity is indicated to be independent of the liquid viscosity. Davies and Taylor further proposed an equation to describe the relationship between the terminal velocity, and the size of the gas bubble, $R_b$, as follows (Ref 25):

$$V_\infty = \sqrt{g\,R_b} \quad \text{as} \quad R_b \geq 2\left(\frac{\sigma}{g\,\rho_f}\right)^{0.5} \quad \text{(Eq 7)}$$

### 2.6 Numerical Procedures

In order to simulate numerically the fluid-flow phenomena in a gas-injected ladle, the following procedures are performed.

1. The ladle system is divided into a number of rectangular elements, called cells.
2. Markers are introduced in the system to represent the existence of the gas bubbles. Gas markers vanish when they exit the system, and new gas markers are added when a new bubble is supposed to appear at the exit of the nozzle based on the gas flow rate and the frequency of bubble formation.
3. The cells are differentiated as full cells, which contain markers and all the neighboring cells all contain markers and at least one of the neighboring cells does not have a marker, and empty cells, which contain no markers.
4. For full cells, the density of each cell is calculated based on the distribution of the gas markers.
5. Solve Eq 1 to 3 in conjunction with the wall-boundary conditions for the velocity and pressure for each full cell.
6. Surface-boundary conditions are used to calculate the velocity and pressure for the surface cells.
7. The velocities of the markers are calculated based on Eq 5, and the new positions of the markers are then calculated based on Eq 6.
8. Return to step 3 until the system reaches the steady state.

## 3. Physical Model

A water-modeling technique was used in this study to simulate physically the fluid-flow phenomena in a gas-injected ladle. A transparent, plexiglass vessel represented the ladle while

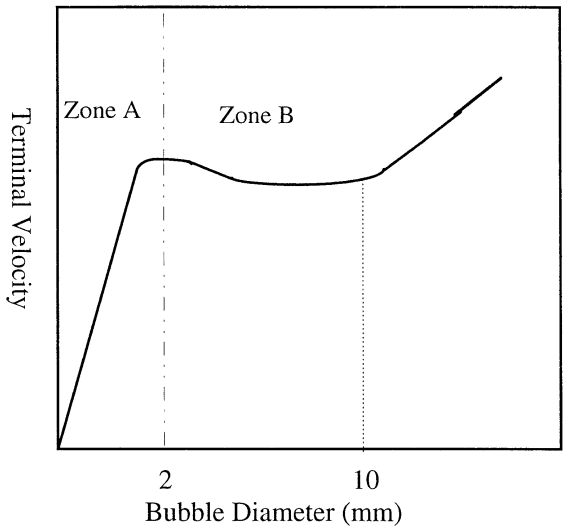


**Fig. 4** Relationship between the terminal velocity of a gas bubble and its size (Ref 17)

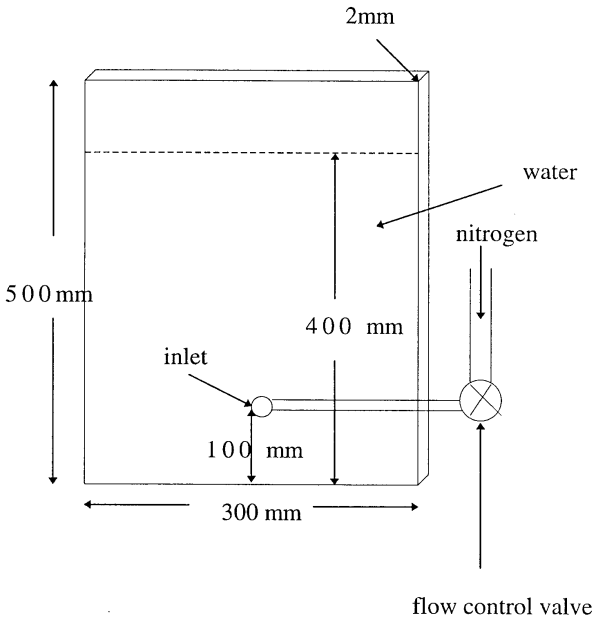


**Fig. 5** Diagram of the two-dimensional ladle constructed in this study

water was used to simulate the molten steel. Nitrogen gas was used in the water model to simulate the argon gas used in the actual injection operation in the steel ladle, which was consistent with the similarity requirement. During the experiment, a series of photographs were taken to examine the shape change of the floating bubble, the rising velocity of the gas bubble, and the interactions among the gas bubbles.

### *3.1 Experimental Setup*

In this study, only two-dimensional analyses were conducted. Therefore, a rectangular vessel as shown in Fig. 5 was constructed as the ladle for the sake of comparison with the numerical simulations. The vessel was 300 mm wide, 500 mm high, and 2 mm thick. A gas introduction tube was inserted in the system, 100 mm above the bottom. A gas flow rate regulating valve was used to control the size of gas bubble formed and the frequency of the gas bubble released.

### *3.2 Experimental Procedures*

To conduct the experiment, the vessel was first filled with water to 400 mm in height. Then, the gas tank was opened to have a predetermined gas flow rate. The control valve was regulated to allow the gas bubbles of desired size and release frequency to form at the outlet of the gas tube. When the fluid-flow system reached the steady state, the fluid-flow phenomenon was recorded using a video camera. The video recording was then carefully examined, and the rising velocities of the gas bubbles were measured. Photographs were also taken from the video recording to investigate the shape variation of the gas bubble during its flotation and the interactions among the various bubbles.

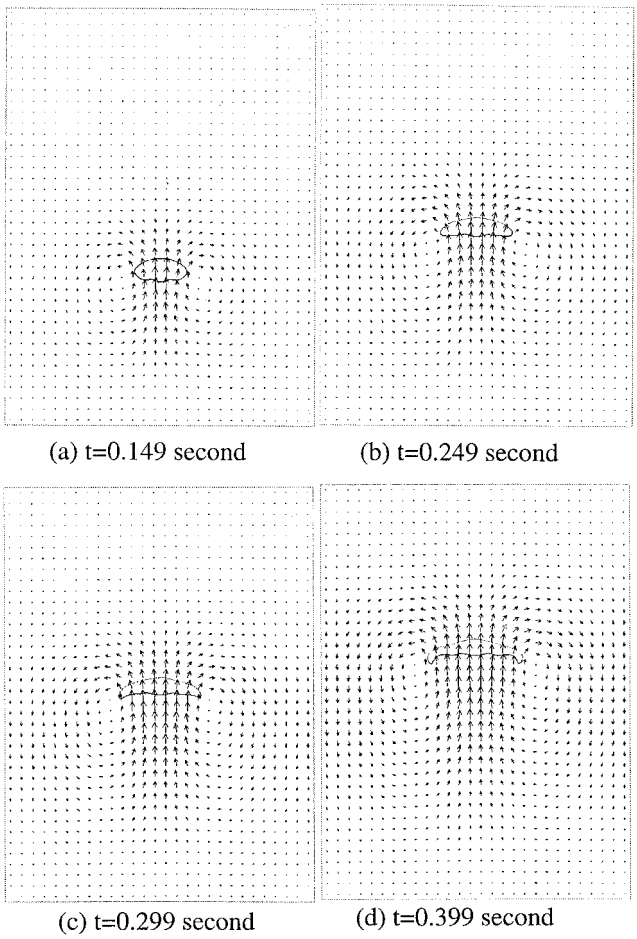


**Fig. 6** Numerically simulated results showing the induced flow field of the liquid and the shape change of the floating bubble for four instants

## 4. Results and Discussion

In this study, a mathematical model has been developed to simulate numerically the interactions between gas bubbles and molten steel during the gas-injection treatment in secondary refining of steel. The current capability of the model is restricted to two-dimensional analyses. The mathematical model was then tested on a water-test bed that was 300 mm wide, 500 mm high, 2 mm thick, and the liquid was filled up to 400 mm high. The gas bubbles were introduced into the system at the centerline and 100 mm above the bottom. The densities of the liquid and the gas were taken to be 1.0 and 0.0012 g/cm$^3$, respectively, in this study. The concerned phenomena included the flow field of the liquid induced by the flotation of the gas bubbles, the shape change of the bubbles during the flotation under the influence of the liquid flow, and the terminal velocities of the gas bubbles. For numerical simulation purposes, the ladle was divided into a 30 by 40 mesh system.

### *4.1 Gas/Liquid Interactions with Only One Gas Bubble in the Ladle*

The model was first tested on the two-dimensional ladle with only one gas bubble to float from the bottom to the top to test the capability of the model to handle the interaction between the relatively large bubble and the liquid. The first bub-

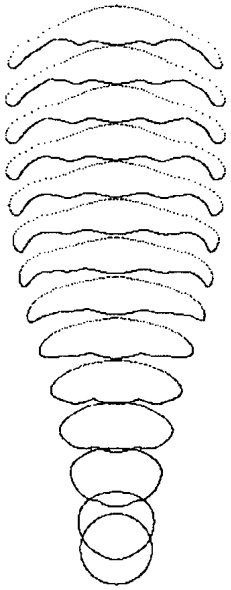

**Fig. 7** Variation of bubble shape during the flotation of a gas bubble of 26 mm in diameter

ble size tested was 26 mm in diameter. The numerically simulated results showing the induced flow field of the liquid and the shape change of the floating bubble for four instants can be seen in Fig. 6. Figure 6(a) shows that a gas bubble rises because the gas is much lighter than the liquid and a buoyancy force is exerted on the bubble. As the bubble floats, it drags the liquid nearby to flow. A negative pressure region exists underneath the gas bubble. Meanwhile, the rising gas bubble is distorted under the influence of the liquid pressure. Figure 6(b) shows that two liquid-flow circulations are induced symmetrically along the track of the bubble movement and the gas bubble is squeezed and distorted. Figure 6(c) shows that as the gas bubble rises higher, the gas bubble is further suppressed in the vertical direction and elongated in the horizontal direction. Eventually, as the buoyancy force balances the drag force, the gas bubble reaches its terminal velocity, and its shape becomes like a spherical cap, as shown in Fig. 6(d). Figure 7 shows exclusively only the shape variation of the bubble of 26 mm in diameter during its flotation.

Different bubble sizes were then tested. They were 10, 30, 40, and 50 mm in diameter. It was found that the induced flow field in the liquid and the shape change of the gas bubble were similar to the previous case. The various terminal velocities for the different bubble sizes can also be obtained for later discussion.

Water-modeling experiments were then conducted. The gas flow rate was regulated to allow only one bubble with various sizes to float in the vessel. The floating phenomena were recorded and later analyzed. Pictures demonstrating the flotation conditions are shown in Fig. 8 and 9 for gas bubble sizes of 26 and 50 mm, respectively. Comparing the numerically simulated results to those of the water-modeling studies shows that the shape-variation characteristics are very much alike. The terminal velocities for the various bubble sizes obtained from the numerical simulations, the water-modeling experiments, and Eq 7 are shown in Fig. 10. It can be seen from the figure that the consistency is very satisfactory.

### *4.2 Gas/Liquid Interactions with Gas Bubbles Continuously Released in the Ladle*

After the developed model had been proven capable of handling the interactions between a relatively large bubble and the liquid, the model was then tested on the same ladle with gas bubbles continuously released from the bottom, which reflects the actual gas-injection operation more realistically. The bubble size was again 26 mm in diameter and one gas bubble was released every 0.27 s. Figure 11 shows the numerically simulated results of the induced flow field of the liquid, the shape

**(a)** **(b)** **(c)**

**Fig. 8** Flotation conditions in water for three instants for the gas bubble size of 26 mm

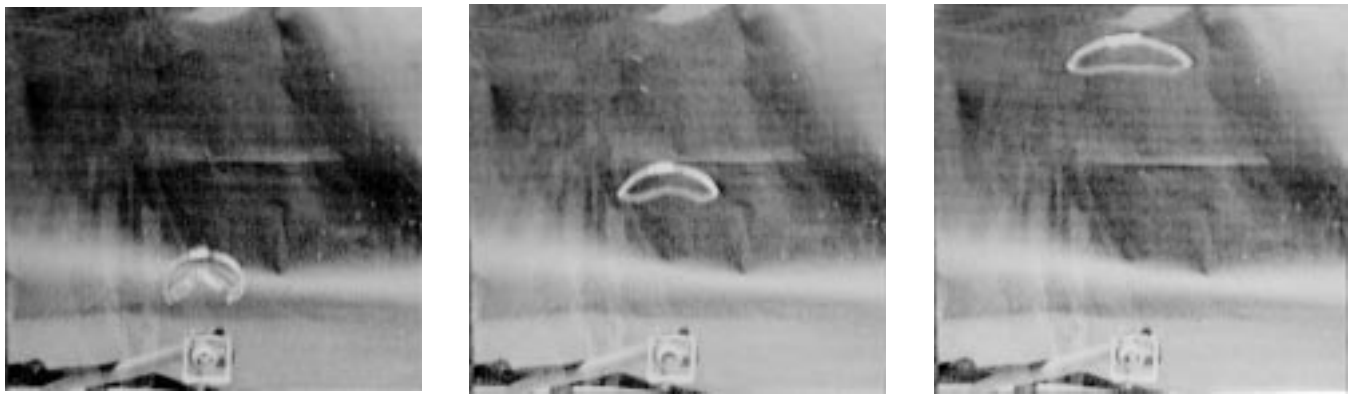

**(a)** **(b)** **(c)**

**Fig. 9** Flotation conditions in water for three instants for the gas bubble size of 50 mm

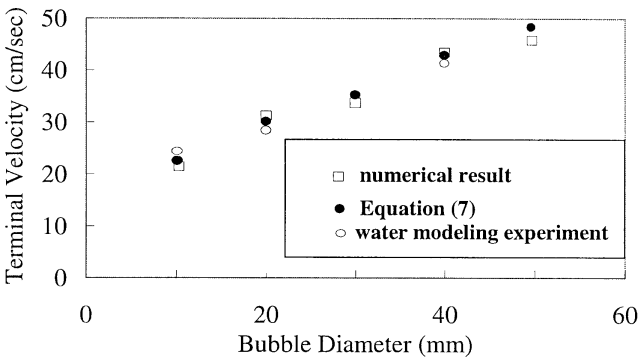


**Fig. 10** Relationship between the terminal velocity and the diameter of the gas bubble as obtained from the numerical results (open squares), the water-modeling experiments (open circles), and Eq 7 (closed circles)

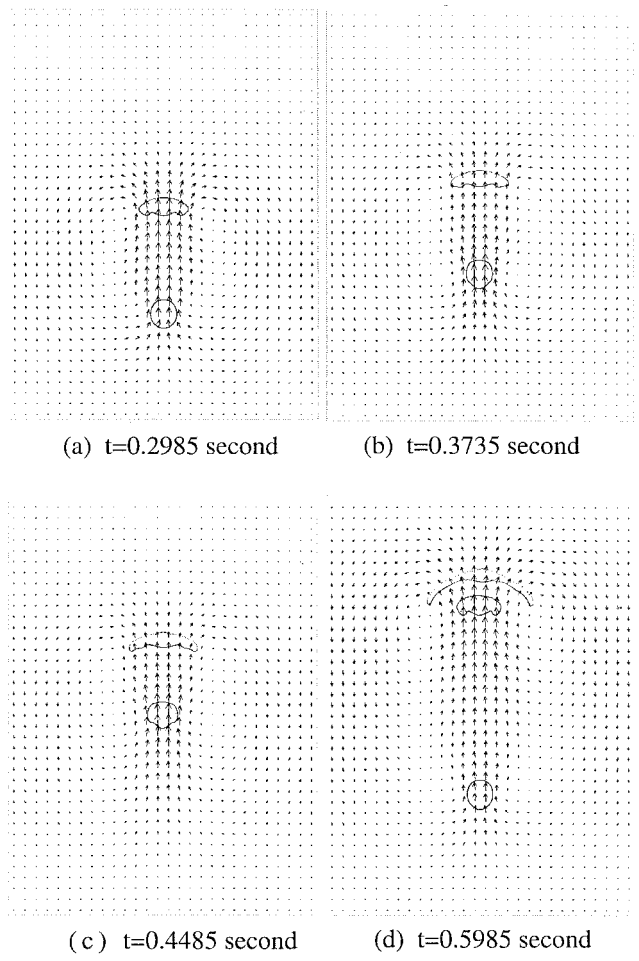


**Fig. 11** Numerically simulated results showing the induced flow field of the liquid, the shape change of the various bubbles, and the interactions among the various bubbles

change of the various bubbles, and the interactions among the various bubbles.

As the first bubble rises, its floating and dragging actions cause the nearby liquid to flow. Everything happens in the same way as in the one-bubble test before the second bubble appears, as shown in Fig. 11(a). The flow from the second bubble is very different from that of the first one. From Fig. 11(b) and (c), it can be seen that the second bubble is elongated in the vertical direction rather than the horizontal direction due to the negative pressure underneath the first bubble created by its flow. The induced flow field in the liquid is also quite different from the first case. The second bubble can be seen to rise faster, presumably due to the negative pressure region underneath the first bubble. The second bubble soon catches up with the first one. Figure 11(d) shows that right before the first two bubbles collide and the third bubble appears, the first bubble has the shape of a spherical cap and the second bubble is also squeezed and becomes flattened, although the extent of the flattening is less. As the second bubble rises very fast, it is fairly far from the bottom as the third bubble appears. The flow behavior of the third bubble is then very much like the first one and the flow of the fourth bubble is very much like the second one. It can be said that for the gas bubbles continuously released, the gas bubbles can be grouped. In this particular case, two bubbles are in a group. The bubbles in one group behave very differently from one another due to their interactions. However, the second group behaves very similarly to the first group, and the phenomenon is repeated group after group.

Again, a water-modeling experiment was conducted. The gas flow rate was regulated to allow gas bubbles of approximately 25 mm diameter to be released in a frequency of approximately one bubble for every 0.27 s. The floating phenomena were again recorded and are shown in Fig. 12. As the numerically simulated results are compared to those of the water-modeling studies, Fig. 12(b) corresponds very well to Fig. 11(b) as far as the shapes of the two bubbles are concerned. Figure 12(c) shows that the second bubble rises very fast and catches up with the first one, which is also consistent with the results shown in Fig. 11(d).

## 5. Conclusions

In this study, a mathematical model based on a computational fluid dynamics technique called marker-and-cell (MAC) was developed to simulate numerically the interactions between gas bubbles and molten steel during the gas-injection treatment in secondary refining of steel. A water model with a plexiglass vessel injected with nitrogen gas was also constructed to simulate physically the gas-injection operation. Photographic observation was used to compare the numerical simulation to evaluate the reliability of the mathematical model. The concerned phenomena included how the flotation of released bubbles induces the liquid to flow, how the shape of the bubbles vary during the flotation under the influence of the liquid flow, and how the various bubbles interact with one another. The bubbles released in this particular treatment were relatively large and very difficult to handle mathematically.

The developed mathematical model was then applied to a two-dimensional ladle with only one bubble rising from the bottom to the top. The simulated results show that during the bubble flotation, the gas bubble gradually becomes flattened and eventually is evolved into a spherical-cap bubble. Liquid

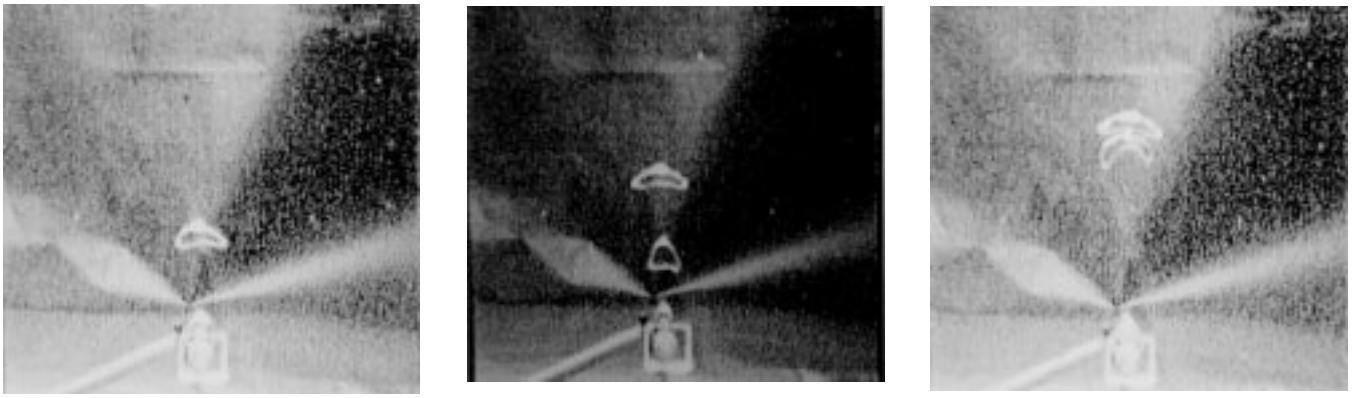

**(a)** **(b)** **(c)**

**Fig. 12** Flotation conditions for the gas bubbles of approximately 25 mm in diameter being continuously released in a frequency of approximately one bubble for every 0.27 s

near the rising bubble is induced to flow and forms two circulations near the tail of the bubble, which are symmetrical with respect to the pathline of the bubble. These phenomena are confirmed by the experimental observations form the water model.

The model was then tested on the same ladle with bubbles continuously released from the bottom. The simulated results show that the first bubble rises in a similar way as the previous case. However, the second bubble is affected by the flow condition underneath the first bubble and becomes slightly elongated in the vertical direction rather than the horizontal direction. The second bubble also rises faster and later collides with the first bubble. The released bubbles can be grouped in clusters. The behaviors of the gas bubbles repeat themselves cluster after cluster. Water-model experiments of the same conditions were also conducted, and the observations are consistent with the results of the numerical simulations.

## Acknowledgment

The authors would like to thank the National Science Council of the Republic of China for the financial support of this study under contract No. NSC 83-0405-E006-050.

## References

1. L.E.K. Holappa, Review of Ladle Metallurgy, *Proc. SCANINJECT II Conf.* (Lulea, Sweden), MEFOS, 1980, p 1:1-1:23
2. A. Nicholson and T. Gladman, *Overview—Non-metallic Inclusions and Developments in Secondary Steelmaking,* The Institute of Metals, 1986
3. J. Szekely, H.J. Wang, and K.M. Kiser, Flow Pattern and Velocity Prediction in a Water Model of an Argon Stirred Ladle, *Metall. Trans.,* Vol 13B, 1976, p 287-295
4. J.H. Grevet, J. Szekely, and N.E. El-Kaddah, An Experimental and Theoretical Study of Gas Bubble Driven Circulation System, *Int. J. Heat Mass Transfer,* Vol 25, 1982, p 487-497
5. Y. Sahai and R.I.L. Guthrie, Hydrodynamics of Gas Stirred Melts, *Metall. Trans.,* Vol 13B, 1982, p 193-211
6. J.S. Woo, J. Szekely, A.H. Castillejos, and J.K. Brimacombe, A Study on the Mathematical Modelling of Turbulent Recirculating Flows in Gas-Stirred Ladles, *Metall. Trans.,* Vol 21B, 1990, p 269-277
7. S.T. Johansen and F. Boysan, Fluid Dynamics in Bubble-Stirred Ladle, *Metall. Trans.,* Vol 19B, 1988, p 755-764
8. D. Mazumdar and R.I.L. Guthrie, An Assessment of Two Phase Calculation Procedure for Hydrodynamic Modelling of Submerged Gas Injection in Ladles, *ISIJ Int.,* Vol 34 (No. 5), 1994, p 384-392
9. M.R. Davidson, Numerical Calculations of Two-Phase Flow in a Liquid Bath with Bottom Gas Injection: The Central Plume, *Appl. Math. Modelling,* Vol 14, 1990, p 67-76
10. M. Iguchi, K. Nozawa, and Z. Morita, Bubble Characteristics in the Momentum Region of Air-Water Vertical Bubbling Jet, *ISIJ Int.,* Vol 31, 1991, p 952-959
11. J.K. Walters and J.F. Davison, The Initial Motion of a Gas Bubble Formed in an Inviscid Liquid, *J. Fluid Mech.,* Vol 12, 1962, p 408-417
12. J.R. Grace, Shapes and Velocities of Bubbles Rising in Infinite Liquids, *Trans. Inst. Chem. Eng.,* Vol 51, 1973, p 116
13. J.R. Grace, T. Wairegi, and T.H. Nguyen, Shapes and Velocities of Single Drops and Bubbles Moving Freely through Immiscible Liquids, *Trans. Inst. Chem. Eng.,* Vol 54, 1976, p 767
14. A.H. Castillejos and J.K. Brimacombe, Measurement of Physical Characteristics of Bubbles Gas-Liquid Plumes: Part II. Local Properties of Turbulent Air-Water Plumes in Vertically Injected Jets, *Metall. Trans.,* Vol 18B, 1987, p 659-671
15. M. Zhou and J.K. Brimacombe, Critical Fluid-Flow Phenomenon in a Gas-Stirred Ladle, *Metall. Trans.,* Vol 25B, 1994, p 681-693
16. M. Iguchi, H. Kawabata, Y. Ito, K. Nakajima, and Z. Morita, Continuous Measurements of Bubble Characteristics in a Molten Iron Bath with Ar Gas Injection, *ISIJ Int.,* Vol 34 (No. 12), 1994, p 980-985
17. W.L. Haberman and R.K. Morton, David W. Taylor Model Basin Rep., 1953, p 802
18. S.M. Pan, J.D. Chiang, and W.S. Hwang, Effects of Gas Injection Condition on Mixing Efficiency in the Ladle Refining Process, *J. Mater. Eng. Perform.,* Vol 6 (No. 1), 1997, p 113-117
19. J.D. Bugg and R.D. Rowe, Modelling the Initial Motion of Large Cylindrical and Spherical Bubbles, *Int. J. Numer. Meth. Fluids,* Vol 13, 1991, p 109-129
20. A. Tomiyama, A. Sou, H. Minagawa, and T. Sakaguchi, Numerical Analysis of a Single Bubble by VOF Method, *JSME Int. J.,* Vol 36B, 1993, p 51-56
21. S.O. Unverdi and G. Tryggvason, A Front-Tracking Method for Viscous, Incompressible, Multi-Fluid Flows, *J. Comput. Phys.,* Vol 100, 1992, p 25-37

22. M. Sussman, P. Smereka, and S. Osher, A Level Set Approach for Computing Solutions to Incompressible Two-Phase Flow, *J. Comput. Phys.*, Vol 114, 1994, p 146-159

23. A. Nishihara, S. Kieda, and Y. Kunugi, Numerical Analysis of the Motion of a Bubble Using MAC Method, *Proc. Jpn. Mech. Soc.*, Vol 59B (No. 562), 1993, p 126-130

24. J.E. Welch, F.H. Harlow, J.P. Shannon, and B.J. Daly, "The MAC Method—A Computing Technique for Solving Viscous, Incompressible, Transient Fluid Flow Problems Involving Free Surfaces," Tech Report LA-3425, Los Alamos Scientific Laboratory, 1966

25. R.M. Davies and G.I. Taylor, *Proc. R. Soc. (London) A*, Vol 200, 1950, p 375-390